

# IMPACT OF THERMAL ASSISTANCE ON SILVER DIFFUSION IN INDIUM SULFIDE THIN FILMS

Meril Mathew<sup>1</sup>, C. Sudha<sup>2</sup> K. P. Vijayakumar<sup>3</sup>

<sup>1</sup> Department of Physics, St. Joseph's College, Devagiri, Kozhikode-673008(India)

<sup>2</sup> Department of Physics, Cochin University of Science and Technology, Kochi-682 022,(India)

## ABSTRACT

Silver coatings on  $\beta$ -In<sub>2</sub>S<sub>3</sub> films have shown anomalous diffusion and doping and thus enhancing the efficiency of indium sulfide as a buffer layer. This paper describes the impact of thermal assistance on silver diffusion in indium sulfide films prepared by chemical spray pyrolysis. The silver doped films were post annealed at two different temperatures and the variations in structural, electrical, and optical properties of these films were studied. It was observed that doping  $\beta$ -In<sub>2</sub>S<sub>3</sub> film with optimum amount of silver modified the structural and electrical properties of the films favorably to enhance the efficiency of indium sulfide as a buffer layer. The quantity of silver required for optimum performance decreased with post annealing treatment.

**Keywords:** Indium sulfide, Silver doping, Spray pyrolysis, Thin film solar cells

## I. INTRODUCTION

The substitution of cadmium sulfide buffer layers by alternative materials is among the challenges of the Cu(In,Ga)(S,Se)<sub>2</sub> thin films based solar cells community since the end of 1990s. The III–VI semiconductor, In<sub>2</sub>S<sub>3</sub> has been a potential alternative due to its opto-electronic properties. With optimal physical properties, this semiconductor material can meet the requirements of window material or buffer layer in thin film solar cells [1-4] due to its stability, wide band gap and photoconductivity [5]. In<sub>2</sub>S<sub>3</sub> can be used as an effective nontoxic substitute for cadmium sulfide (CdS) in Copper Indium Gallium Sulfide (CIGS) based solar cells. The motivation for using In<sub>2</sub>S<sub>3</sub> as a buffer layer in CIGS solar cells is not only to eliminate toxic cadmium, but also to improve light transmission in the blue wavelength region by using a material having band gap wider than that of CdS. CIGS based solar cells, with In<sub>2</sub>S<sub>3</sub> as the buffer layer could reach efficiencies (16.4 %) near to those obtained by devices made with standard CdS buffer layer [6].

$\beta$ -In<sub>2</sub>S<sub>3</sub> belongs to A<sub>2</sub><sup>III</sup>B<sub>3</sub><sup>II</sup> compounds which represent solids having large concentration of vacancies and yet with completely satisfied chemical bonds [7, 8]. The ordered modification can, therefore, be interpreted as a quasi-ternary compound, consisting of In, S and ‘vacancies’. In this material, eight of the twelve tetrahedral sites are occupied by indium and other four are empty (the latter are ordered). All octahedral sites are occupied by In and could be written as In<sub>6</sub>(In<sub>2</sub>□)S<sub>12</sub>, where □ indicates vacancies and parenthesis describes tetrahedral site [8, 9]. Due to large number of cationic vacancies indium sulfide acts as a “sink” for many guest atoms.

There are only very few works have been reported on doping of In<sub>2</sub>S<sub>3</sub> films, so as to modify its structural and electrical properties. Becker et al. reported that doping of In<sub>2</sub>S<sub>3</sub> films with Sn resulted in samples with low resistance [9]. Kim et al. reported that doping of indium sulfide single crystals with cobalt, lead to the decrease of structural defects [10]. N. Kamoun et al. reported that presence of Al caused an increase in adsorption of



oxygen in the sample [11]. Roland Diehl and Rudolf Nitsche [12], reported stabilization of  $\gamma$ - $\text{In}_2\text{S}_3$ , (which is the high temperature phase of  $\text{In}_2\text{S}_3$ ) at room temperature through replacing about 5 to 10% of In atoms by As, Sb or Bi. N. Barreau et al. reported that incorporation of Na resulted in wider band gap and better conductivity [13].

We have reported the anomalous effect of silver diffusion in indium sulfide [14]. From XPS depth profile of the sample, it was seen that on having Ag/ $\text{In}_2\text{S}_3$  structures silver diffused throughout the depth of indium sulfide even without any thermal assistance. Doping  $\beta$ - $\text{In}_2\text{S}_3$  thin films with Ag resulted in samples with enhanced crystallinity and grain size. It was observed that there was an optimum amount of Ag doping and further increase in doping concentration showed retracing effects. Electrical resistivity of the films decreased drastically from  $1.2 \times 10^3 \text{ } \Omega\text{cm}$  to  $0.06 \text{ } \Omega\text{cm}$  due to doping. Sample having optimum doping was found to be more photosensitive and low resistive when compared with pristine sample. This is an anomalous effect because usually it is observed with decreased resistivity (high dark current) the photosensitivity of the films would decrease. This anomalous effect of having high photosensitivity and low resistivity is the contribution of defect level created by doping. These films exhibited photoluminescence at room temperature from sub bandgap donor acceptor pair transition. This is a near band gap emission for the absorber layers and have the potential of improving the efficiency of the solar cells. Improvement in crystallinity, conductivity and photosensitivity due to doping of spray pyrolysed  $\text{In}_2\text{S}_3$  films with Ag helped to attain efficiency of 9.5% for Ag/ $\text{In}_2\text{S}_3$ /CuIn<sub>2</sub>/ITO (indium tin oxide) cell [1].

In this paper we are discussing the post deposition annealing effects of these Ag/ $\text{In}_2\text{S}_3$  samples. Post annealing treatment was done to understand the impact of annealing on the samples as the diffusivity of silver in indium sulfide could be increased with thermal assistance.

## II. EXPERIMENTAL DETAILS

$\text{In}_2\text{S}_3$  thin films were deposited on soda lime glass substrate using Chemical Spray Pyrolysis (CSP) technique. Spraying solution was made up of indium chloride ( $\text{InCl}_3$ ) and thio-urea ( $\text{CS}(\text{NH}_2)_2$ ) in the required molarities. The solution was sprayed on a substrate kept at a temp of  $300 \pm 5 \text{ } ^\circ\text{C}$ , administered at a spray rate of 20 ml/min. The total volume of the solution sprayed was 200 ml and the thickness was  $0.5 \mu\text{m}$  with indium to sulfur ratio in the solution at 1.2/8. This ratio was selected as it showed the maximum photosensitivity and yielded nearly stoichiometric films [2]. In order to dope these samples with silver, thin layer of silver was deposited over the  $\text{In}_2\text{S}_3$  layer, using vacuum evaporation technique (pressure during evaporation was  $\sim 2 \times 10^{-5} \text{ m bar}$ ). A minor rise in temperature (12 K) was observed during the silver deposition. Different masses of silver {3 mg (1 nm), 5 mg (1.7 nm), 10 mg (3.4 nm), 12 mg (4 nm) and 15 mg (5.1 nm)} were evaporated for doping different sets of  $\text{In}_2\text{S}_3$  films. These doped samples were named as IS:3Ag, IS:5Ag, IS:10Ag, IS:12Ag, IS:15Ag respectively and pristine sample was named as IS. In order to understand the effect of thermal assistance on diffusion, the films were annealed at  $100^\circ\text{C}$  and  $200^\circ\text{C}$  for one hour in vacuum ( $\sim 2 \times 10^{-5} \text{ m bar}$ ) after silver coating. These annealed samples were named as IS: (*mass of silver evaporated*) Ag (*annealing temperature in  $^\circ\text{C}$* ).

Structural properties of pristine and Ag doped  $\text{In}_2\text{S}_3$  films were determined by means of X-ray Diffraction (XRD), (Rigaku-D. Max.C-X-ray diffractometer having, Cu  $\text{K}_\alpha$  radiation of wavelength  $\lambda = 1.5405 \text{ } \text{Å}$ ). Morphological studies were done with the help of Scanning Electron Microscope (SEM) (Cambridge Model). X-ray Photoelectron Spectroscopy (XPS), (ULVAC- PHI unit, Model: ESCA 5600 CIM) capable of employing

argon ion sputtering, was used to obtain the depth profile and atomic ratio of the films. Optical properties were obtained from optical absorption spectra (UV-VIS-NIR spectrophotometer-JASCO V-570 model). Dark and illuminated conductivities were measured with the help of two-probe technique. Photosensitivity  $[(I_L - I_D)/I_D]$ , where  $I_L$  is current under illumination and  $I_D$  is the dark current] measurements were performed using Keithley 236 Source Measure Unit. For the photocurrent measurement, the sample was illuminated with a tungsten halogen lamp ( $60 \text{ mW/cm}^2$ ). Electrical contacts were given using silver paint, in the form of two end contacts, having a distance of 5 mm between them.

### III. RESULTS AND DISCUSSION

#### 3.1 Structure and morphology

XRD patterns of the annealed (i.e., post annealed after silver diffusion) samples showed a clear improvement in crystallinity up to an optimum amount of doping and after that a retracing phenomenon was observed. This observation is quite similar to variation in XRD with silver diffusion at room temperature [14].

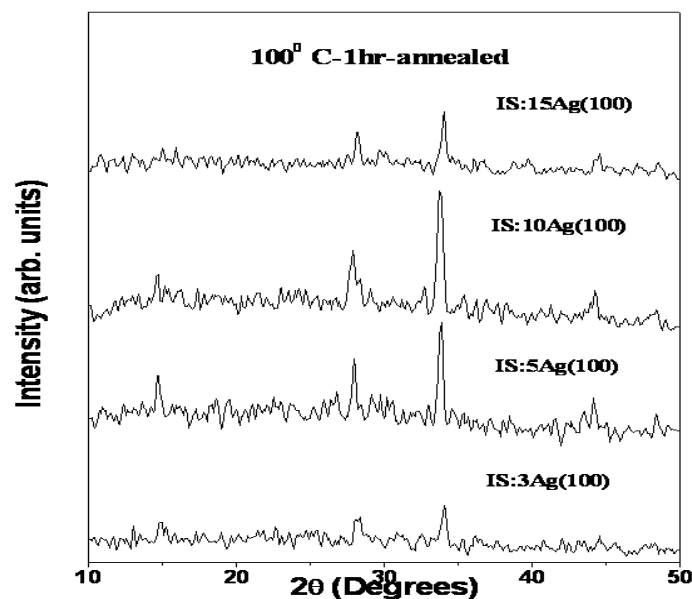
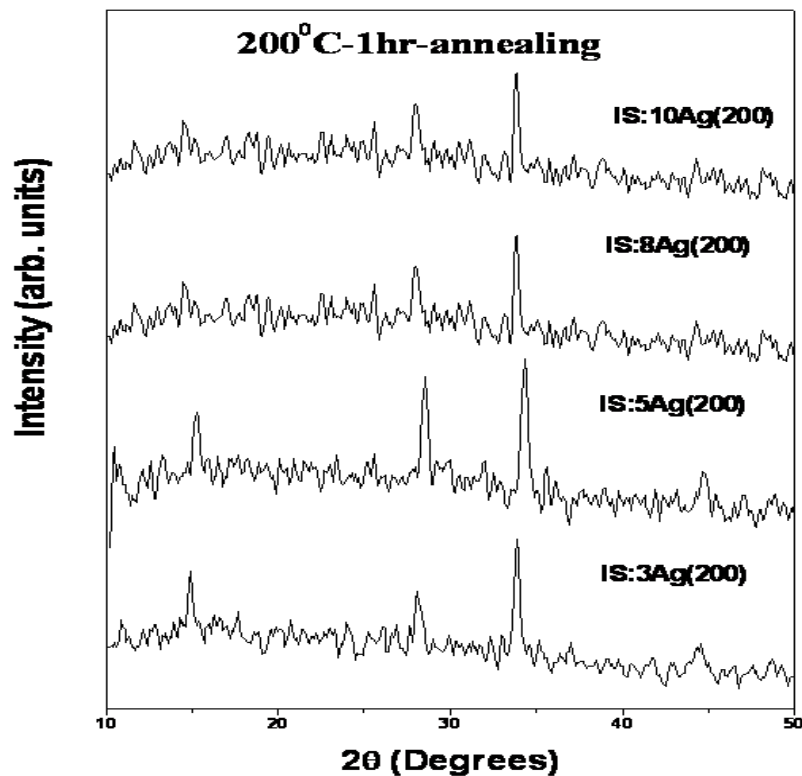


Fig. 1 variation of XRD of doped samples post annealed at  $100^\circ\text{C}$  for 1hour

However it was seen that the quantity of silver needed for optimum performance decreased with thermal assistance. In silver diffused films with no post annealing, the crystallinity increased up to sample IS:12Ag and started decreasing from IS:15Ag [14]. For the samples which have undergone annealing at  $100^\circ\text{C}$  for one hour, the optimum value of silver [up to which the crystallinity improved] decreased to 10 mg. i.e. for IS:10Ag(100) as seen in figure1 and for the samples which have undergone annealing at  $200^\circ\text{C}$  for one hour the optimum value decreased to 5 mg i.e. IS:5Ag(200) as seen in figure2. The thermal assistance might be enhancing the silver diffusion, there by decreasing required quantity for optimum performance (Table 1).



**Fig. 2 XRD of doped samples, annealed at 200°C after Ag deposition.**

The  $d$  values coincided with that of  $\beta$ - $\text{In}_2\text{S}_3$  in standard JCPDS data card (25-390). It is of note that there is no new phase indicating that the post annealing treatments of silver doped indium sulfide thin films do not change the structure of  $\text{In}_2\text{S}_3$  nor result in the formation of any new crystalline compounds. As in the case of silver doped samples, the peak positions slightly shifted to lower values of  $2\theta$  on annealing. Correspondingly, value of lattice spacing ( $d$ ) increased [14]. This proved that lattice parameters increased with silver deposition; but with annealing, this Debye Scherrer formula also showed a marginal increase with annealing. The grain size of optimum doped samples at different annealing temperatures is tabulated in Table 1. occurred at relatively lower percentage of silver. The  $c/a$  ratio was nearly constant for all samples. Grain size calculated using

**Table I. Properties of optimum sample with annealing**

	Un annealed	100°C annealed	200°C annealed
Optimum Quantity	12 mg	8 mg	5 mg
Grain size (nm)	36.87	37.76	39.48
Band gap (eV)	2.24	2.2	2.19
Resistivity ( $\Omega$ cm)	50.5	38.82	26.24
Photosensitivity	538.88	235.84	118.25

XPS depth profile of the annealed samples proved that diffusivity of silver enhanced due to the thermal process. Interestingly it was observed that on achieving optimum value at lower doping levels, annealing sourced the

excess silver to retrace to the surface of the films (Figure 3). Comparison of figure 4 (XPS of optimum doped sample without post annealing (IS:12Ag)) with figure 3, the depth profile XPS analysis of the same sample with post annealing at 200<sup>0</sup>C for 1hr gives a clear picture of retracing of excess silver to the film surface with annealing. From XRD analysis the optimum quantity of silver at 200<sup>0</sup>C post annealing was found to be 5 mg i.e., IS:5Ag(200), and excess silver could have retraced to surface layers. In this case, quantity of silver accommodated at vacant cationic and interstitial sites would have reached optimum level at a relatively lower amount of silver on increasing the diffusion by thermal assistance. Binding energies of indium and sulfur indicated the formation of indium sulfide (162.5 eV for S2p, 444.9 eV and 452.9 eV for In3d<sub>5/2</sub> and In3d<sub>3/2</sub> respectively) and were in agreement with the reported values [15].The Sulfur concentration decreased with silver doping [14].

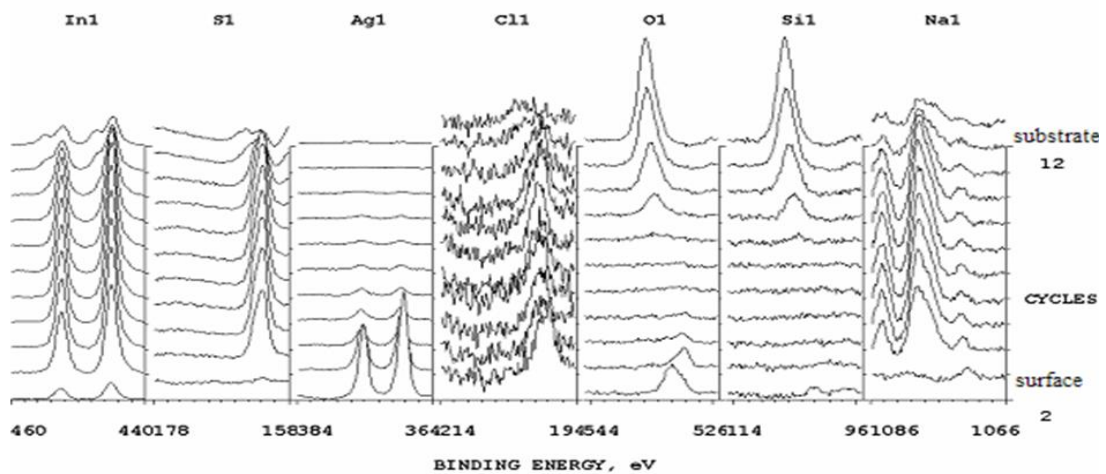


Fig.3 XPS depth profile of sample IS:12Ag (200<sup>0</sup> annealed)

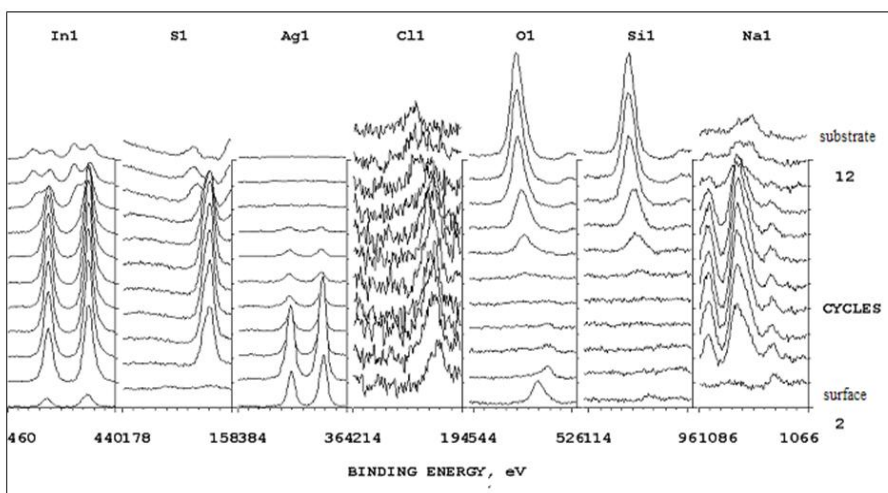
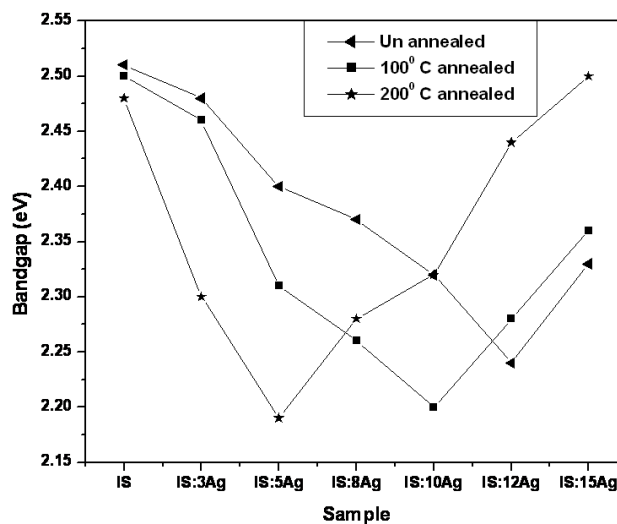


Fig.4. XPS depth profile of sample IS:12Ag

Oxygen was again present as a surface contaminant (532.5 eV). Towards the interior of the film, intensity of the peak corresponding to oxygen decreased and there was a shift in peak position, indicating the presence of metal oxide (530.5 eV for O 1s in In<sub>2</sub>O<sub>3</sub>) [5]. The Oxygen concentration increased on annealing. Correspondingly

there was a decrease in the peak height of sulfur at the surface of the doped samples indicating a decrease in atomic percentage. Chlorine was also present throughout the depth of the sample. Presence of sodium observed, could be due to the diffusion from glass substrate during spraying, as it was done at 573 K.

### 3.2. Optical studies



**Fig. 5 Variation of bandgap on annealing**

Optical absorption spectra, was recorded in the wavelength region 190 -1200 nm. The optical band gap was determined from  $(\alpha h\nu)^2$  vs.  $h\nu$  graph . Band gap of pristine sample decreased from 2.51 eV to 2.48 eV with annealing. This could be due to the improvement in crystallinity observed during annealing in the pristine films. For the doped samples the band gap decreased up to optimum doping and after that the retracing (band gap increased) behavior was observed. On annealed samples also the nature of optical behavior remained same (Fig.5). But the individual performance of the samples changed on annealing. Lowest band gap was 2.19 eV for IS:5Ag (200).

The decrease in band gap up to optimum doping concentration can be due to the increase in crystallinity and decrease in sulfur concentration. [10, 16] But on increasing the doping concentration above the optimum value, the band gap showed a retracing effect (i.e. increasing). This could be due to the decrease in crystallinity and presence of oxygen in the sample, forming metal oxide. XPS studies revealed a sudden increase in oxygen concentration and formation of metal oxide when doping concentration increased beyond the optimum value. N. Barreau et al. [17] has reported increase in band gap with oxygen concentration.

### 3.3. Electrical studies

Resistivity of the pristine sample also decreased on annealing. It was seen from the XRD analysis that the overall crystallinity of the samples increased with annealing and hence the decrease in resistivity on annealing could be assumed to be due to this. In general, the resistivity of annealed samples was lower than that of the unannealed ones.

For doped samples it was observed that resistivity of the samples decreased with doping but a small rise in resistivity was observed towards optimum value. And after the optimum value a sharp decrease in resistivity is

observed. Doped samples preserved the same electrical behavior even at different post annealing temperatures as revealed in figure 6. But the optimum value changed with annealing as revealed by structural and optical studies. Our earlier studies [14] have proved that defect created by doping is responsible for this anomalous electrical behavior. The defect analysis done using photoluminescence, dark conductivity and temperature stimulated current measurements showed that increase in indium interstitials due to doping accounts for the low resistivity of the samples. It was observed that, at low doping concentration, silver atoms were positioned in the ordered vacancy sites (activation energy ~ 1.2 eV). At still higher doping concentration [close to optimum doping] silver atoms were setting into indium sites creating an acceptor level (activation energy ~ 0.6 eV) resulting in a small increase in resistivity. On further increase in doping concentration, silver atoms got into interstitial positions resulting in the drastic decrease in resistivity.

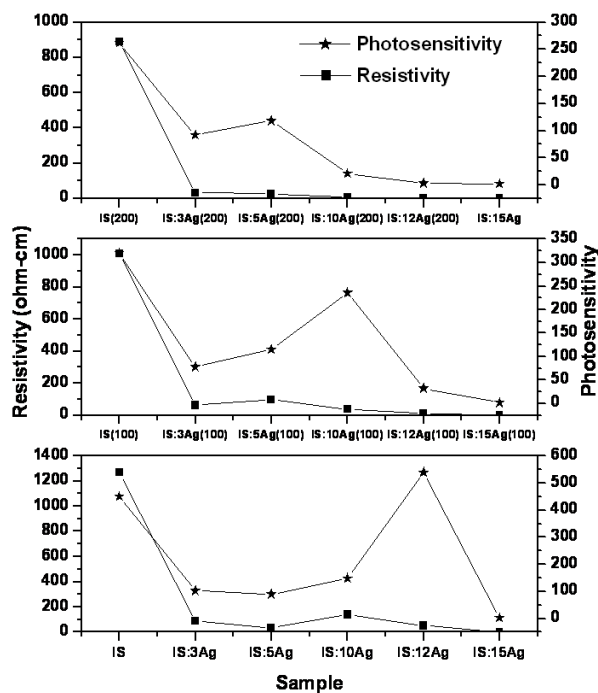


Fig. 6 Variation of electrical properties with annealing

Photosensitivity was found to be more for unannealed samples. The photosensitivity is in accordance with dark conductance value. For annealed samples, resistivity decreased, increasing the dark current of the samples thereby diminishing the photosensitivity. Among doped samples photosensitivity was high for optimum doped samples (Table 1). Usually a decrease in photoconductivity was observed with the decrease in resistivity, but here on the contrary, optimum doped sample showed an increased photosensitivity in spite of its low resistivity. The enhanced photosensitivity of this sample was due to the contribution of the acceptor level created by Ag doping as reported earlier [14]. The holes generated by the acceptors might have reduced the majority carrier density slightly, (resulting in considerable reduction of minority carrier loss due to recombination). This might have enhanced the photosensitivity even though the sample had low resistivity, making the sample extremely suitable for photovoltaic application as evident from our own work [1].

**VI. CONCLUSION**

Doping  $\beta$ - $\text{In}_2\text{S}_3$  thin films (prepared using CSP technique) with Ag resulted in samples with enhanced crystallinity and grain size. From XPS depth profile of the sample, it could be seen that silver diffused throughout the depth even without annealing. It was observed that there was an optimum amount of Ag, required for doping and further increase in doping concentration showed retracing effects. Annealing treatment on doped films could bring down the quantity of silver deposited for optimum performance. Doping  $\beta$ - $\text{In}_2\text{S}_3$  film with optimum amount of silver modified the structural and electrical properties of the films favorably to enhance the efficiency of buffer layer. Though annealing increased the crystallinity of the films, doped films with no post deposition treatments showed a better electrical performance.

**REFERENCE**

- [1] T. T. John, Meril Mathew, C. Sudha Kartha, K. P. Vijayakumar, T. Abe, Y. Kashiwaba (2005)  $\text{CuInS}_2/\text{In}_2\text{S}_3$  thin film solar cell using spray pyrolysis technique having 9.5% efficiency. *Sol. Energy. Mat. Sol. Cells*, 89(1):27-36.
- [2] T. T. John, S. Bini, Y. Kashiwaba, T. Abe, Y. Yasuhiro, C. Sudha Kartha and K. P. Vijayakumar (2003) Characterization of spray pyrolysed indium sulfide thin films, *Semiconductor Science and Technology*. 18 (6): 491-500
- [3] Paul O Brien, David J. Octway and John R. Walsh (1998) Novel precursors for the growth of  $\alpha$ - $\text{In}_2\text{S}_3$ : trisdialkyldithiocarbamates of indium. *Thin Solid Films*, 315:57-61.
- [4] M. Amlouk, M. A. Ben Said, N. Kamoun, S. Belgacem, N. Brunet and D. Barjon (1999) Acoustic properties of  $\beta$ - $\text{In}_2\text{S}_3$  thin films prepared by spray., *Jpn. J. Appl. Phys.* 38:26-30.
- [5] L. Bhira, H. Essaidi, S. Belgacem, G. Couturier, J. Salardenne, N. Barreaux and J. C. Bernède (2000) Structural and Photoelectrical Properties of Sprayed  $\beta$ - $\text{In}_2\text{S}_3$  Thin Films. *Phys. Stat. Sol. (a)* 181:427-435.
- [6] N. Naghavi, S. Spiering, M. Powalla, B. Cavana and D. Lincot (2003) High-Efficiency Copper Indium Gallium Diselenide (CIGS) Solar Cells with Indium Sulfide Buffer Layers Deposited by Atomic Layer Chemical Vapor Deposition (ALCVD). *Prog. Photovolt: Res. Appl.* 11(7):437-443.
- [7] K. Kambas, J. Spyridelis and M. Balkanski (1981) Far infrared and Raman optical study of  $\alpha$ - and  $\beta$ - $\text{In}_2\text{S}_3$  compounds. *Phys. Status Solidi B*. 105(1):291-296
- [8] N.Barreau (2009) Indium sulfide and relatives in the world of photovoltaics, *Solar Energy*, 83(3):363-371.
- [9] R. S. Becker, T. Zheng, J. Elton and M. Saeki (1986) Synthesis and photoelectrochemistry of  $\text{In}_2\text{S}_3$ . *Solar Energy Mater.* 13(2):97-107.
- [10] W. T. Kim, W. S. Lee, C. S. Chung and C. D. Kim (1988) Optical properties of  $\text{In}_2\text{S}_3:\text{Co}^{2+}$  single crystals. *J. Appl. Phys.* 63(11):5472-5475.
- [11] N. Kamoun, S. Belgacem, M. Amlouk, R. Bennaceur, J. Bonnet, F. Touhari, M. Nouaoura and L. Lassabatere (2001) Structure, surface composition, and electronic properties of  $\beta$ - $\text{In}_2\text{S}_3$  and  $\beta$ - $\text{In}_{2-x}\text{Al}_x\text{S}_3$ . *J. Appl. Phys.* 89(5): 2766-2771.
- [12] Diehl R and Nitsche R (1973) Vapour and flux growth of  $\gamma$ - $\text{In}_2\text{S}_3$ , a new modification of indium sesquisulphide. *J. Cryst. Growth*. 20(1):38-46.





- [13] N. Barreau, J. C. Bernede, C. Deudon, L. Brohan, S. Marsillac (2002) Study of the new  $\beta$ -In<sub>2</sub>S<sub>3</sub> containing Na thin films Part I: Synthesis and structural characterization of the material. J. Cryst. Growth. 241(1-2):4-14
- [14] Meril Mathew, R.Jayakrishnan, P.M.Ratheesh Kumar, C.Sudha Kartha, Y.Kashiwaba, T.Abe and K.P.Vijayakumar (2006) Anomalous behavior of silver doped indium sulfide thin films. J. Appl. Phys. 100(3):33504-1-8
- [15] Shu-Hong Yu, Lei Shu, Yong-Sheng Wu, Jian Yang, Yi Xie and Yi-Tai Qian (1999) Organothermal synthesis and characterization of nanocrystalline  $\beta$ -indium sulfide. J. Am. Ceram. Soc. 82(2):457-60.
- [16] J. George, K. S. Joseph, B. Pradeep and T. I. Palson, (1988) Reactively evaporated films of indium sulphide. Phys. Status Solidi A. 106:123.
- [17] N. Barreau, S. Marsillac, D. Albertini, J. C. Bernede (2002) Structural, optical and electrical properties of  $\beta$ -In<sub>2</sub>S<sub>3-3x</sub>O<sub>3x</sub> thin films obtained by PVD. Thin Solid Films 403-40